CHAPTER 124

# 2DH COMPUTATION OF TRANSIENT SEA BED EVOLUTIONS

Huib J. de Vriend*

## ABSTRACT

The interaction between the constituent models for waves, currents, sediment transport and bottom level changes in a class of compound 2DH mathematical models of transient sea bed evolutions in the coastal zone is investigated mathematically, using the theory of characteristics and a harmonic analysis technique. This leads to contrary indications as to the importance of including diffraction in the wave model and to the unambiguous conclusion that the bottom slope effect on the sediment transport is indespensable for the mathematical system to be inherently stable. This conclusion is shown to imply that depth-integrated current model are insufficient to describe the flow in this type of morphological computations for the nearshore zone or complex coastal areas.

## INTRODUCTION

In recent years, the progress in the physical understanding and the mathematical modelling of the water and sediment motion in coastal areas has enabled the numerical simulation of these phenomena to become a widely applied and useful tool in coastal hydraulics and coastal zone management. Besides, they seem to have brought the mathematical modelling of the integrated effect of these phenomena, the 3D morphological evolution of the sea bed, within reach. Various research institutes, all over the world, are making substantial research efforts in this field (see e.g. Fleming et al., 1976; Watanabe, 1982; Coeffé et al., 1982; McAnally et al., 1984; Yamaguchi et al., 1984; De Vriend, 1987a,b).
One of the cornerstones in the development of mathematical models of transient sea bed evolutions is a thorough physical knowledge, of the elementary phenomena tide, waves, currents, sediment motion and sedimentation/erosion, as well as their interactions (also see De Vriend, 1987a). The present paper attempts to contribute to this last field of knowledge, which still exhibits significant lacunae.
After the description and the mathematical formulation of the class of models to be considered, the interaction between the constituent models is analysed mathematically and the sensitivity of the model to some major simplifications in the constituents is assessed. Finally, conclusions are drawn on the applicabitlity.

## GENERAL OUTLINE OF THE MODELS

The models concern 3D transient morphological evolutions in coastal areas. Basic elements are depth-integrated wave and current models, local sediment transport formulae and the sediment balance.

*Delft Hydraulic Lab., Delft, The Netherlands

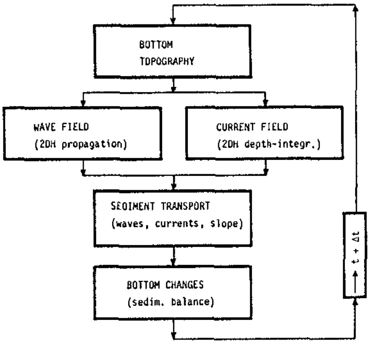


Fig. 1 Flow chart of investigated models

Fig. 1 gives an aggregate flow chart of the interconnection of these elements. Although the present analysis concerns systems of differential equations and the behaviour of their solutions, this flow chart also pertains to their elaboration in a numerical model, so that it can be considered as describing a computational procedure.

Fig. 1 shows that the constituent models are connected in series, with feedback via the bed topography only. This is a simplification of reality, as it ignores other feedback mechanisms, such as current refraction. On the other hand, it focuses attention on the morphological interaction to be investigated.

Another important simplification is the absence of wave dissipation. This means that wave-driven currents are left out of consideration as a mechanism through which the waves can interact with the other components of the system. The principal remaining interaction mechanism for the waves is the stirring of sediment. From a practical point of view, this is a fairly limitative assumption, but on the other hand the interaction analysis should be built up step by step. After the analysis for currents alone (De Vriend, 1987a,b), this is another step on a much longer way to go.

## WAVE MODEL

The most general formulation of the wave models to be considered is based on the mild-slope equation for linear monochromatic unidirectional gravity waves (Berkhoff, 1976). Ignoring current refraction and dissipation, this equation can be written as

$$\frac{\partial}{\partial x}\left(cc_g\frac{\partial \Psi}{\partial x}\right)+\frac{\partial}{\partial y}\left(cc_g\frac{\partial \Psi}{\partial y}\right)+k^2\,cc_g\Psi=0 \qquad (1)$$

in which: $x$, $y$ = cartesian co-ordinates in the horizontal plane,
$c$ = phase celerity of the waves,
$c_g$ = group celerity of the waves,
$k$ = wave number and
$\Psi$ = complex wave potential.

Substitution of the wave-type expression

$$\Psi(x,y)=\mathrm{Re}\left[a(x,y)\exp\left\{i\Phi(x,y)\right\}\right] \qquad (2)$$

in which $i=\sqrt{(-1)}$ and the amplitude and phase functions $a(x,y)$ and $\Phi(x,y)$ are real, leads to the eikonal equation

$$\left(\frac{\partial \Phi}{\partial x}\right)^2+\left(\frac{\partial \Phi}{\partial y}\right)^2=k^2+\frac{1}{cc_g a}\left[\frac{\partial(cc_g)}{\partial x}\frac{\partial a}{\partial x}+\frac{\partial(cc_g)}{\partial y}\frac{\partial a}{\partial y}\right]+\frac{1}{a}\left[\frac{\partial^2 a}{\partial x^2}+\frac{\partial^2 a}{\partial y^2}\right] \qquad (3)$$

and the transport equation

$$\frac{\partial}{\partial x}\left(cc_g a^2 \frac{\partial\Phi}{\partial x}\right) + \frac{\partial}{\partial y}\left(cc_g a^2 \frac{\partial\Phi}{\partial y}\right) = 0 \tag{4}$$

For purely refracting wave fields (geometric optics approximation), the last two terms of (3) drop out and the equations can be reduced to (also see Appendix I)

$$\frac{\partial}{\partial x}(k \sin\Theta) - \frac{\partial}{\partial y}(k \cos\Theta) = 0 \tag{5}$$

$$\frac{\partial}{\partial x}(E\, c_g \cos\Theta) + \frac{\partial}{\partial y}(E\, c_g \sin\Theta) = 0 \tag{6}$$

in which $\Theta$ denotes the direction of wave propagation and $E = \frac{1}{2}\rho g a^2$ is the energy density of the wave field.
Both the complete refraction/diffraction equations (3) and (4) and the refraction equations (5) and (6) will be investigated in their interaction with the other components of the model.

## CURRENT MODEL

In order to avoid unnecessary complications, the current model includes a number of simplifying assumptions, most of which can be shown to have no essential influence on the interaction (De Vriend, 1985):

- depth-integrated formulation in terms of depth-averaged velocities,
- almost-parallel flow (no secondary currents),
- rigid-lid approximation for the free surface,
- no horizontal diffusion or dispersion of momentum,
- no wave influence on the bottom shear stress,
- bottom shear stress acting in the depth-averaged flow direction,
- no coriolis acceleration,
- no external driving forces, and
- steady flow.

Under these assumption, the flow model can be written as

$$u\frac{\partial u}{\partial x} + v\frac{\partial u}{\partial y} = -\frac{1}{\rho}\frac{\partial p}{\partial x} - \frac{\tau_{bx}}{\rho h} \tag{7}$$

$$u\frac{\partial v}{\partial x} + v\frac{\partial v}{\partial y} = -\frac{1}{\rho}\frac{\partial p}{\partial y} - \frac{\tau_{by}}{\rho h} \tag{8}$$

$$\frac{\partial u}{\partial x} + \frac{\partial v}{\partial y} + u\frac{\partial h}{\partial x} + v\frac{\partial h}{\partial y} = 0 \tag{9}$$

in which:

| | | |
|---|---|---|
| $u$, $v$ | = | depth-averaged velocity components |
| $p$ | = | total pressure (piezometric head * spec. weight) |
| $\rho$ | = | mass density of the fluid |
| $h$ | = | water depth |
| $\tau_{bx}$, $\tau_{by}$ | = | bottom shear stress components. |

For the system of equations to be closed, the bottom shear stress has to be related to the other dependent variables in the system. The present analysis requires no further specification than

$$\frac{\tau_{bx}}{\rho h} = ru; \quad \frac{\tau_{by}}{\rho h} = rv \quad \text{with} \quad r = \text{fnct}(u_t, h); \quad u_t = (u^2 + v^2)^{\frac{1}{2}} \tag{10}$$

The flow model (7) through (10) will only be considered in its complete form, as the effects of simplifications have been investigated before (De Vriend, 1985 and 1987a).

## SEDIMENT TRANSPORT MODEL

As was stated before, the sediment transport model is basically restricted to sediment transport formulae. Especially in coastal areas, where a large part of the transported sediment is suspended load, this can be a rather limitative assumption, though not necessarily fatal (c.f. Van Banning et al., 1987). Nevertheless, this type of model is choses, not only from the step-by-step philosophy, but also because transport formulae are widely used in practice. All the same, systems including suspended load models remain to be investigated (cf. Lin et al., 1984).
In addition to this restriction, it is assumed that, apart from the bottom slope effect,

- the magnitude of the transport is a function of the current velocity, the water depth and the wave height (and possibly other quantities that are not figuring as dependent variables in the present system),
- the direction of the transport coincides with the depth-averaged flow direction, and
- the magnitude of the transport is independent of the derivatives of the dependent variables.

This leads to the following mathematical formulation of the transport without bottom slope effect;

$$S'_x = \frac{u}{u_t} S'_t \;;\; S'_y = \frac{v}{u_t} S'_t \text{ with } S'_t = \text{fnct}\,(u_t, h, E) \tag{11}$$

in which $S'_x$ and $S'_y$ are the components of the transport vector and $S'_t$ denotes its magnitude.
The near-bottom sediment transport is influenced by the bottom slope, via the downslope gravitational force, acting on the bed load, and via the vertical component of the near-bed velocity, acting on the suspended load. These effects can be incorporated via the following approximative adjustments (cf. Koch et al., 1981 and Bailard, 1981):

$$S_t = S'_t\,(1-\beta_1 \frac{\partial z_b}{\partial s}) \text{ and } \tan\alpha \triangleq \frac{S_y}{S_x} = \tan\delta - \beta_2 \frac{\partial z_b}{\partial n} \tag{12}$$

in which $z_b$ denotes the bottom level, and s and n are stream-oriented and stream-normal horizontal co-ordinates (metric), respectively; $\delta$ is the depth-averaged flow direction.
Depending on the transport concept, the factors $\beta_1$ and $\beta_2$ are equal (Bailard, 1981) or not (Koch et al., 1981) and vary with the wave and current parameters. For simplicity, they are chosen equal and constant, i.e. $\beta_1 = \beta_2 = \beta$, so that (11) and (12) can be elaborated to

$$S_x = S'_t\,(\cos\delta - \beta \frac{\partial z_b}{\partial x}) \text{ and } S_y = S'_t\,(\sin\delta - \beta \frac{\partial z_b}{\partial y}) \tag{13}$$

provided that the bottom slopes are small compared with $\beta^{-1}$.

## BOTTOM LEVEL CHANGES

The rate of change of the bottom level follows from the conservation of sediment mass

$$(1 - \varepsilon_p) \frac{\partial z_b}{\partial t} + \frac{\partial S_x}{\partial x} + \frac{\partial S_y}{\partial y} = 0 \tag{14}$$

in which $\varepsilon_p$ denotes the porosity of the bottom. This part of the model is quite unambiguous and, if combined with a transport formula, leaves no room for alternative formulations.

LINEARIZATION OF THE SYSTEM

Equations (3), (4), (7) through (10), (11), (13) and (14) basically from the mathematical model equations, although additional expressions have to be given for c, $c_g$, k, h, r and $S_t'$ in terms of the dependent variables $\Phi$ (or $\Theta$), a (or E), u, v , p and $z_b$. It is not necessary, however, to have these expressions explicity. The analysis of the system concerns the linearized equations in the vicinity of an arbitrary point in the solution space. If the values of the dependent variables at this point are indicated by the suffix "o", a non-linear relation like the sediment transport formula, for instance, is approximated by

$$S_t'(u_t,h,E) \approx S_{t_o}' + (u_t - u_{t_o}) \left.\frac{\partial S_t'}{\partial u_t}\right|_o + (h-h_o) \left.\frac{\partial S_t'}{\partial h}\right|_o + (E-E_o) \left.\frac{\partial S_t'}{\partial E}\right|_o \qquad (15)$$

For each of the non-linear additional expressions, it is sufficient to specify the derivatives with respect to the relevant dependent variables.

After some elaboration of the equations, the most convenient way to specify the necessary quantities of this type turns out to be the specification of

$$T_1 \triangleq \frac{1}{1-\varepsilon_p}\left[\frac{h}{S_t'}\frac{\partial S_t'}{\partial h} - 1\right] \; ; \; T_2 \triangleq \frac{1}{1-\varepsilon_p}\left[\frac{u_t}{S_t'}\frac{\partial S_t'}{\partial u_t} - 1\right] \; ; \; T_3 \triangleq \frac{1}{1-\varepsilon_p}\frac{a}{S_t'}\frac{\partial S_t}{\partial a} \qquad (16a)$$

$$C_h \triangleq \frac{h}{c}\frac{dc}{dh} \; ; \; C_{gh} \triangleq \frac{h}{c_g}\frac{dc_g}{dh} \; ; \; R_u \triangleq \frac{u_t}{r}\frac{\partial r}{\partial u_t} \; ; \; R_h = \frac{h}{r}\frac{\partial r}{\partial h} \qquad (16b)$$

Since the wave number in the present wave models is inversely proportional to the phase celerity c, the relation between k and h is sufficiently characterized by $k_o$ and $C_h$. Finally, the rigid-lid approximation provides the linear relation

$$h = z_s - z_b \qquad (17)$$

in which $z_s$ is the prescribed elevation of the rigid lid.

Making use of these relations and definitions, and considering $T_1$, $T_2$, $T_3$, $C_h$, $C_{gh}$, $R_u$ and $R_h$ as constants in the vicinity of the point "o", the system of equations can be elaborated as described in Appendix I. The resulting system contains two equations describing how the wave field responds to small changes in the bottom topography, three equations describing how the current field responds to such changes and one equation describing how the bottom elevation responds to small changes in the wave and current fields. This last equation reads (also see: De Vriend, 1987b):

$$\frac{\partial z_b}{\partial t} + (T_2 - T_1)\frac{S_t'}{h}\left[\frac{u}{u_t}\frac{\partial z_b}{\partial x} + \frac{v}{u_t}\frac{\partial z_b}{\partial y}\right] - \beta S_t'\left[\frac{\partial^2 z_b}{\partial x^2} + \frac{\partial^2 z_b}{\partial y^2}\right] + T_2\frac{S_t'}{u_t^3} +$$

$$+ \left[-v^2\frac{\partial u}{\partial x} + uv\frac{\partial u}{\partial y} + uv\frac{\partial v}{\partial x} - v^2\frac{\partial v}{\partial y}\right] + T_3\frac{S_t'}{a}\left[\frac{u}{u_t}\frac{\partial a}{\partial x} + \frac{v}{u_t}\frac{\partial a}{\partial y}\right] = 0 \qquad (18)$$

This can be considered as an advection/diffusion equation for the bottom level, in which the last two terms, representing the effects of the wave and current fields, act as source terms. It shows that the bottom evolution must have a partly propagative, partly diffusive character, the former due to the non-linearity of the transport formula (otherwise the factor $T_2$-$T_1$ equals zero), the latter due to the bottom slope effect on the transport.

CHARACTERISTICS ANALYSIS

The system of equations derived in Appendix I can be analyzed with the theory of characteristics (Courant et al., 1961; also see Flokstra, 1981), which provides information on the elementary behaviour of the bottom changes, such as the celerity of bottom disturbances. Application of this technique to the same system without waves revealed (De Vriend, 1987b), that the bottom evolution has a propagative character if the bottom slope effect on the sediment transport is ignored. Even though in that case the transport is directed exactly downstream, bottom disturbances will not only propagate downstream with the well-known 1D celerity derived by De Vries (1969) and also showing up in Eq. (18): like an elementary disturbance in the water surface of a pond, they will also expand in all directions, in a peculiar star-shaped pattern (see Fig. 2).

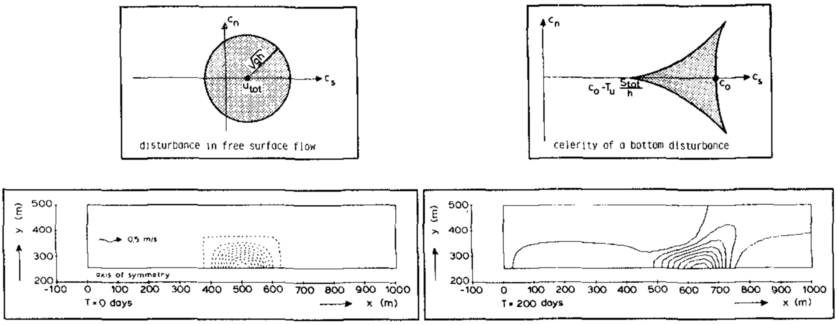


Fig. 2 Celerity patterns in 2DH models. Top left: current and surface wave. Top right: current and alluvial bottom. Bottom: numerical simulation of elementary bottom evolution.

Although formally the propagative character vanishes when the bottom slope effects are included (vide the diffusive character these effects introduce into Eq. (18)), numerical experiments have shown the typical celerity pattern to remain recognizable in the bottom evolution, like it is in the numerical experiment shown in Fig. 2. Therefore, a characteristics analysis with the bottom slope effects disregarded is expected to provide relevant information on the elementary bottom evolution, also in the presence of waves.
Application of the characteristics analysis to the present extensive system is a cumbersome task, which cannot possibly be described here. A detailed description and a discussion of the technique are given in a recent publication by the author (De Vriend, 1987b). Here only some of the results will be given. As the sustaining numerical experiments are awaiting the completion of an appropriate computer program, these results are presented with some reserve.

If the complete mild-slope equation is incorporated in the model, the bottom celerity components with respect to the stream-oriented co-ordinate system are given by

$$c_s = (T_2 - T_1)\frac{S_t'}{h} + T_2\frac{S_t'}{h}\xi;\quad c_n = T_2\frac{S_t'}{h}\eta \tag{19}$$

in which the parameters $\xi$ and $\eta$ are related by

$$\eta^4 + (2\xi^2 - 5\xi - \tfrac{1}{4})\,\eta^2 + \xi\,(\xi + 1)^3 = 0 \tag{20}$$

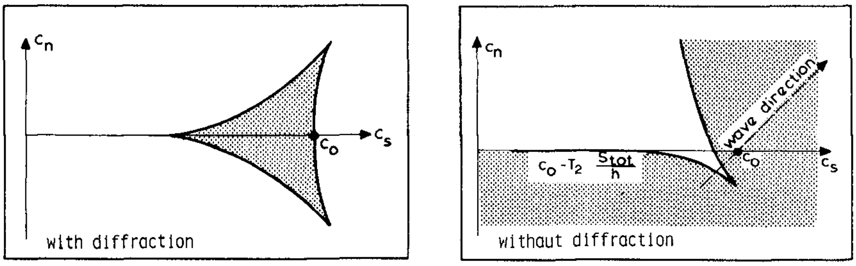


Fig. 3 Influence of wave diffraction on bottom celerities

These expressions, represented graphically in Fig. 3 (left), are exactly the same as for the case without waves. So the celerity is qualitatively independent of the way the sediment transport is influenced by the wave height: $T_3$ does not figure in (19) or (20). Quantitatively, the celerity does depends on the wave height via $S_t'$.
If the sediment transport depends on the angle between the wave and current directions the agreement with the case without waves is disturbed. So the conclusion is sensitive to the type of transport formula.

An entirely different celerity pattern can emerge when using simplified wave models. As this pattern is determined by the highest derivatives of the dependent variables in the various equations, disregarding diffraction leads to an essentially different system in this respect.

With the refraction equations (5) and (6), instead of (3) and (4), the expressions for the bottom celerity components read

$$c_s = (T_2 - T_1)\frac{S_t'}{h} + T_2\frac{S_t'}{h}\xi + \frac{1}{2}C_{gh}T_3\frac{S_t'}{h} + \frac{1}{2}C_hT_3\frac{S_t'}{h}\xi^* \tag{21}$$

$$c_n = T_2\frac{S_t'}{h}\eta + \frac{1}{2}C_h\,T_3\frac{S_t'}{h}\eta^* \tag{22}$$

with the parameters $\xi$, $\eta$, $\xi^*$ and $\eta^*$ related by

$$\xi = (1-X)\,(2X-1) \text{ and } \eta = \pm\, 2\,X\,[X(1-X)]^{\frac{1}{2}} \tag{23}$$

$$\xi^* = X^4\,\frac{X^3(1-X)^3 - [X\xi\,\sin(\Theta-\delta)\,\cos(\Theta-\delta) + \eta\,(1-X)\,\sin^2(\Theta-\delta)]^2}{(1-X)^2\,[X^2\,\cos(\Theta-\delta) + \frac{1}{2}\,\eta\,\sin(\Theta-\delta)]^4} \tag{24}$$

$$\eta^* = 2X^6\,\frac{X\xi\,\sin(\Theta-\delta)\,\cos(\Theta-\delta) + \eta\,(1-X)\,[\sin^2(\Theta-\delta) - \frac{1}{2}]}{(1-X)\,[X^2\,\cos(\Theta-\delta) + \frac{1}{2}\,\eta\,\sin(\Theta-\delta)]^4} \tag{25}$$

in which the parameter X goes through all values between 0 and 1. Note that (23) is equivalent to (20), so that the celerties (21) and (22) consist of two parts, one corresponding with the case without waves and one proportional to $T_3$, the latter also depending on the angle between

the wave and current directions.
Fig. 3 (right) gives an example of this celerity pattern, for

$$T_1 = -2;\ T_2 = 2;\ T_3 = 2;\ C_h = 0.5;\ C_{gh} = 0.375 \text{ and } \Theta-\delta = 45°$$

corresponding with the adapted Engelund-Hansen transport formula (Van de Graaff et al., 1979) and the shallow water wave celerities.
The resulting celerity pattern is essentially different from the one with diffraction included: it is no longer a closed curve and, consequently, the area of influence has become semi-infinite. On closer inspection, this behaviour is related to an essential property of purely refracting wave fields: if a wave ray encounters a bottom disturbance, its entire further course is influenced, and so is the wave height along this part of the ray (see. e.g. Dingemans, 1985).
Caution is required when interpreting these results in terms of applicability of types of wave models in the computation of transient morphological evolutions. The results suggest that a refraction model as described by Eqs. (5) and (6) be not applicable. It has to be noted, however, that the characteristics analysis focuses attention on a single aspect of the bottom evolution, viz. the celerity of small disturbances. It is thinkable that this aspect is irrelevant to certain situations. Only numerical experiments for well-selected test cases can show this.

## HARMONIC ANALYSIS

In addition to the characteristics analysis, a harmonic analysis can be utilized to investigate the interaction between the constituents of a compound morphological model (cf. Deigaard, 1983 and Tsujimoto et al., 1985). It provides information on the propagation and amplification/damping of harmonic bottom waves. In principle, it can be applied to the transient morphological processes, considering the bottom-wave evolution in time, as well as to the equilibrium bottom topography, considering the variation of harmonic modes in space (cf. Struiksma et al., 1985).

So far, the harmonic analysis of the system including wave effects has only been successful for the transient processes. Like the characteristics analysis, this technique considers the linearized system, for simplicity about the point ($\Theta_o$, $a_o$, $u_o$, $v = 0$, $p_o$, $z_b = 0$) in the solution space. The resulting system is given in Appendix I.
The technique of the harmonic analysis is well-known: harmonic perturbations of the type

$$z_b = \hat{z}_b \exp\{i(k_t t + k_x x + k_y y)\} \tag{26}$$

with $k_t$ complex and $k_x$ and $k_y$ real, are substituted into the linearized system of equations, to yield a system in $\hat{\Theta}$, $\hat{a}$, $\hat{u}$, $\hat{v}$, $\hat{p}$ and $\hat{z}_b$, with $k_t$, $k_x$ and $k_y$ as parameters. The condition under which there is a non-trivial solution gives a relation between $k_t$, $k_x$ and $k_y$, from which $k_t$ can be solved if $k_x$ and $k_y$ are given.
In order to have a reference for the wave effects, this technique will first be applied to the system without waves. Without going into the algebraic operations, the result reads

$$\mathrm{Re}(\zeta_c) = \sigma\left\{-1 + \frac{4A_c\sigma^2\nu^2(\sigma^2+\nu^2) + 2B_c\nu^2[\sigma^2 + (1+\mathrm{Ru})\nu^2]}{4\sigma^2(\sigma^2+\nu^2)^2 + [\sigma^2 + (1+\mathrm{Ru})\nu^2]^2}\right\} \tag{27}$$

$$\mathrm{Im}(\zeta_c) = D_c(\sigma^2+\nu^2) + \frac{2A_c\sigma^2\nu^2\ [\sigma^2 + (1+Ru)\nu^2] - 4B_c\sigma^2\nu^2(\sigma^2+\nu^2)}{4\sigma^2\ (\sigma^2+\nu^2)^2 + [\sigma^2 + (1+Ru)\nu^2]^2} \tag{28}$$

with: $$\zeta_c = \frac{k_t}{2(T_2-T_1)r_o}\ ;\ \sigma = \frac{u_o}{2r_o}\,k_x;\ \nu = \frac{u_o}{2r_o}\,k_y \tag{29}$$

$$A_c = \frac{T_2}{T_2-T_1}\ ;\ B_c = \frac{T_2}{T_2-T_1}\,\frac{1+R_u-R_h}{2}\ ;\ D_c = \frac{\beta}{T_2-T_1}\,\frac{2r_oh_o}{u_o} \tag{30}$$

Note that this system contains two important physical length scales (also see Struiksma et al., 1985), viz. the adjustment length of the flow, $\lambda_w$, and the adjustment length of the bottom, $\lambda_s$, given by

$$\lambda_w = \frac{u_o}{2r_o} \quad \text{and} \quad \lambda_s = \beta h_o \tag{31}$$

The second term in the expression for $\mathrm{Im}(\zeta_c)$ is easily shown to be negative if $A_c > 0$, and $R_h < 0$, as is usually the case. This means, that for $D_c = 0$, i.e. in the system without bottom slope effects, all modes are unstable. So this system has no stable solution (cf. De Vriend, 1985).
For $D_c > 0$ (negative values are not realistic), the additional term in (28) is positive, i.e. the bottom slope effect on the sediment transport has a damping effect on bottom disturbances, as it should according to the bottom level equation (18). Besides, the additional term increases with the resultant wave number, so this damping effect will be stronger for shorter waves (which have steeper slopes).
As an example of how this works out quantitatively, Fig. 4 gives a graphical representation of (27) and (28), with and without bottom slope effects. The values of the constants correspond with the Engelund and

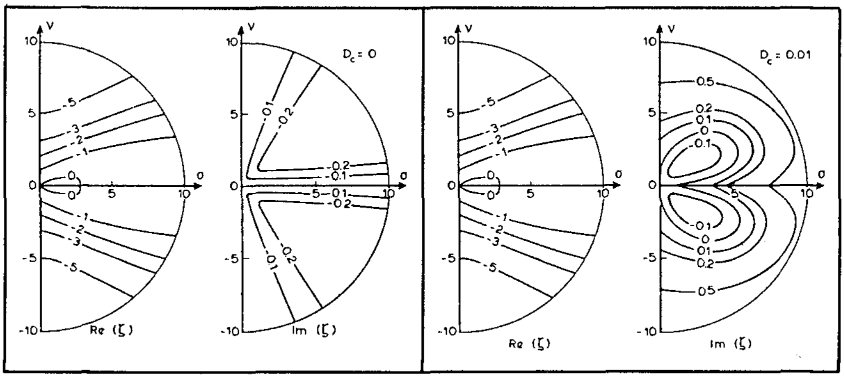


Fig. 4 Initial growth rate of harmonic bottom disturbances (current only)

Hansen transport formula ($T_1 = -1$, $T_2 = 4$) and Chezy's bottom friction law ($R_u = 1$, $R_h = -1$, $r_o = gu_o/[C^2h]$). In the case with bottom slope effects, $D_c$ was chosen 0.01, which corresponds with $\beta \approx 4$. For $D_c = 0$, $\mathrm{Im}(\zeta_c)$ is always negative, indeed, whereas for $D_c \neq 0$, $\mathrm{Im}(\zeta_c)$ is only negative in two relatively small areas, representing fairly long bottom waves. The existence of such unstable modes is not necessarily unrealistic (Deigaard, 1983; also see Struiksma et al., 1985 and De Vriend, 1987a).

When applied to the system including waves, the harmonic analysis yields the following result

$$\mathrm{Re}(\zeta_w) = \sigma\{-1 + \frac{4A_w\, \sigma^2\nu^2(\sigma^2+\nu^2) + 2B_w\, \nu^2[\sigma^2+(1+R_u)\nu^2]}{4\sigma^2(\sigma^2+\nu^2)^2 + [\sigma^2 + (1+R_u)\nu^2]^2} +$$

$$+ \frac{4C_w\gamma^2\chi^2 - E_w(\psi^2 + \chi^2)^2}{4\gamma^2\psi^2-(\psi^2 + \chi^2)^2}\} \tag{32}$$

$$\mathrm{Im}(\zeta_w) = D_w\,(\sigma^2+\nu^2) + \frac{2A_w\, \sigma^2\nu^2[\sigma^2+(1+R_u)\nu^2] - 4B_w\, \sigma^2\nu^2(\sigma^2+\nu^2)}{4\sigma^2(\sigma^2+\nu^2)^2 + {}^5\sigma^2 + (1+R_u)\nu^2]^2} \tag{33}$$

with:

$$\zeta_w = \frac{k_t}{2(T_2-T_1+\frac{1}{2}C_{gh}T_3)r_o}\ ;\ \psi=\sigma\cos\Theta_o+\nu\sin\Theta_o;\ \chi=\sigma\sin\Theta_o-\nu\cos\Theta_o \tag{34}$$

$$A_w = \frac{T_2}{T_2-T_1+\frac{1}{2}C_{gh}T_3}\ ;\ B_w = A_w\frac{1+R_u-R_h}{2};\ D_w = \frac{\beta}{T_2-T_1+\frac{1}{2}C_{gh}T_3}\frac{2r_oh_o}{u_o} \tag{35}$$

$$C_w = \frac{\frac{1}{2}C_hT_3}{T_2-T_1+\frac{1}{2}C_{gh}T_3};\ E_w = \frac{\frac{1}{2}C_{gh}T_3}{T_2-T_1+\frac{1}{2}C_{gh}T_3};\ \gamma = \frac{u_o}{2r_o}k \tag{36}$$

Apart from the coefficients, these expressions are very much the same as in the case without waves: the only difference is an additional term in the expression for $\mathrm{Re}(\zeta)$. This implies that the amplification/damping behaviour of the bottom disturbances remains qualitatively the same, with a predominant role for the bottom slope effects.
As a quantitative example, Fig. 5 gives graphical representations of (33) and (34), without and with bottom slope effects $D_w = 0$ and $D_w = 0.01$,
respectively), without and with diffraction ($\gamma = 0$ and $\gamma = 30$, respectively).
The values of the constants are chosen the same as in the example in Fig. 3, viz. $T_1=-2$, $T_2=2$, $T_3=2$, $C_h=0.5$, $C_{gh}=0.375$, but now with $\Theta_o=0°$ (waves and current in the same direction) and with $R_u=1$ and $R_h=-1$ (Chezy). Apparently, the diffraction effect on $\mathrm{Re}(\zeta_w)$ is rather small, especially for the longer modes.
These results suggest that the incorporation of diffraction in the wave model should have a minor effect on the elementary behaviour of bottom disturbances. However, caution should be exercised, again, when interpreting these results in terms of applicability of types of wave models. The analysis focuses attention on the evolution of small harmonic bottom perturbations, starting from the linearized system of equations. Besides, the indication it gives is contrary to the one given by the characteristics analysis. This does not imply that the two analyses yield contradictory results, since they consider different aspects (amplitude behaviour and propagation behaviour, respectively). Which of these aspects is decisive for the sensitivity of the model to diffraction is still not clear. Numerical model tests and further research are needed in order to arrive at definite conclusions.

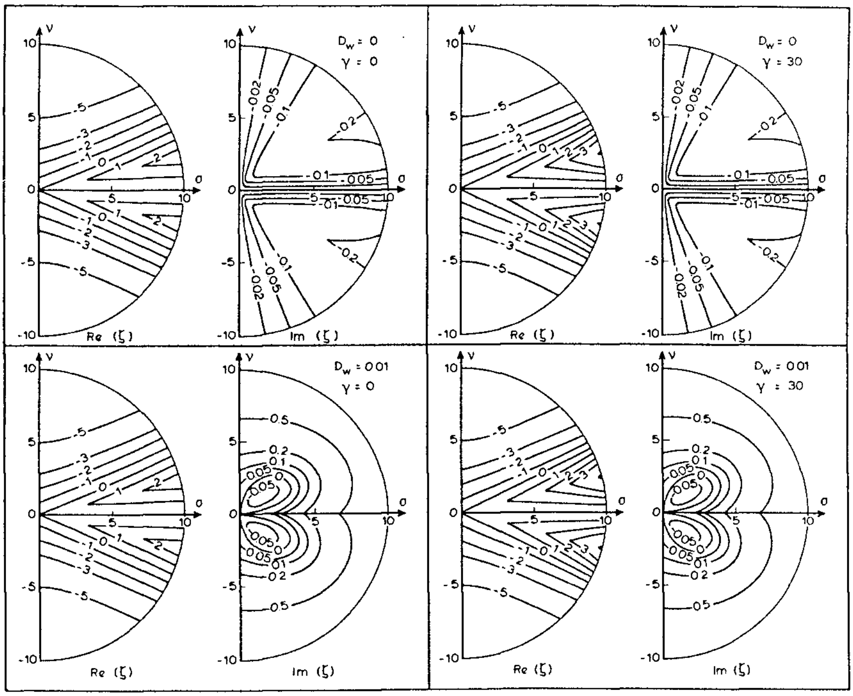

Fig. 5 Influence of wave diffraction on initial growth rate (waves + currents)

DISCUSSION

The investigated system, though including the principal interacting constituents (waves, currents, sediment transport, bottom level changes), is still a highly simplified representation of reality. For instance, the interaction via the response of wave breaking and the induced currents to morphological changes is left out of consideration. Especially in the surf zone, this seems to be an interaction of primary importance.

Nevertheless, the present analyses are practically relevant. If the dissipation of wave energy by breaking is formulated according to Battjes et al., (1978) and the corresponding driving forces per unit area are taken proportional to the dissipation density divided by the phase celerity (Longuet-Higgins, 1970; Dingemans et al., 1987), the relevant terms in the wave and current models are easily shown not to contain the highest derivatives of the dependent variables. Hence this interaction has no effect on the bottom celerity pattern found from the characteristics analysis. The harmonic analysis with this interaction included is still in progress, but is has already become clear that the bottom slope effect on the sediment transport is still a major (if not the only) damping agent in the system.

Another limitation of the present work is, that only linearized systems are considered. When there is a better outlook on the composition and the validity of mathematical models of transient 3D sea bed evolutions, their non-linear behaviour, including the possibility of bifurcations and chaotic behaviour, will have to be investigated.

The harmonic analysis of all variants and extensions of the model that have been investigated so far, clearly indicates that the bottom slope effect on the sediment transport is indispensable in the computation of transient morphological evolutions. If this slope-reducing mechanism is included, however, also the principal slope-generating mechanisms have to be taken into account, if it were only not to wind up with a zero beach slope.

In the nearshore zone, the onshore transport due to the asymmetry of the near-bottom orbital motion is a major slope-generating agent, as appears from investigations of coastal profile evolutions (Stive, 1986; De Vriend, 1986). A fascinating corroboration of this statement, though for edge waves instead of sea or swell, was given by Holman et al. (1982).

On the other hand, the wave-induced undertow in the surf zone causes an off-shore, so usually down-slope transport that is mostly stronger than the asymmetry-induced on-shore transport there (De Vriend et al., 1986). So, once the asymmetry-induced transport is included in a model of near-shore morphological evolutions, the transport due to the undertow, and hence the undertow itself, cannot be left out of consideration. This means that a depth-integrated current model is not sufficient for this kind of situations.

In most of the practical applications, the model area extends beyond the nearshore. Outside the surf zone, the undertow is absent and the waves induce only a much weaker drift current. The asymmetry-induced transport is found wherever the waves "feel" the bottom (so usually in large parts of the model), but it decreases as the water depth increases. This does not imply, that at deeper water the bottom slope effect is the only remaining cross-stream mechanism and that, consequently, a depth-integrated current model suffices. In the complex situations to which 2DH models use to be applied, the flow is curved almost as a matter of course. Besides, sand coasts without strong winds are rare and the coriolis-effect is present almost everywhere. Hence secondary flows due to wind, curvature and the coriolis-effect will occur and exert their influence on the sediment transport and the morphological changes. So in these cases the application of depth-integrated current models is disputable, as well.

This negative conclusion regarding depth-integrated current models does not mean that 2DH flow computation facilities are useless for morphological computations. Experience with river bend modelling (Struiksma et al., 1985) and recent investigations on the modelling of 3D nearshore currents (De Vriend et al., 1986) make clear, that without too limitative assumptions, the flow can be described with a standard depth-integrated model, extended with a simple profile technique for the secondary flow.

## CONCLUSIONS

The two methods used to analyse the interaction between the constituents of the present class of compound 2DH mathematical models of transient sea bed evolutions yield contrary indications on the importance of diffraction in the wave model.

The harmonic analysis unambiguously shows, that the bottom slope effect on the sediment transport (via gravitation and via vertical advection) is indispensable for inherent stability of the mathematical system.
The necessity to include this bottom slope effect implies, that the influence of the asymmetry of the wave-induced orbital motion and of secondary flows has to be taken into account, as well. Consequently, depth-integrated current models are insufficient to describe the flow in models of 3D morphological evolutions, in the nearshore zone and in complex coastal areas.
Depth-integrated current models extended with a simple profile technique to describe the secondary flow appear to be suited for this kind of applications.

ACKNOWLEDGEMENTS

The investigations described herein were part of the TOW Coastal Research Programme, financed by the Netherlands Government and conducted jointly by the Ministry of Transport and Public Works (Rijkswaterstaat), Delft Hydraulics and the Technical University Delft. The author gratefully acknowledges Mr. M.W. Dingemans for his lessons in wave-field theory.

REFERENCES

**Bailard, J.A.**, 1981. An energetics total load sediment transport model for a plane sloping beach. J. Geoph. Res., 86, no. C11, p. 10938-10954.
**Battjes, J.A. and Janssen, J.P.F.M.**, 1978. Energy loss and set-up due to breaking of random waves. Proc. 16th ICCE, Hamburg, p.569-587.
**Berkhoff, J.C.W.**, 1976. Mathematical models for simple harmonic linear water waves; wave diffraction and refraction. Delft Univ. of Techn., Doct. thesis, 103 pp. (Also: Delf Hydr. Lab., Publ. no 163.).
**Bijker, E.W.**, 1971. Longshore transport computations. Proc. ASCE, J. of the Waterways, Harbours and Coastal Engineering Division, WW4, p.687-701.
**Coeffé, Y., Péchon, Ph.**, 1982. Modelling of sea-bed evolution under wave action. Proc. 18th ICCE, Capetown, p. 1149-1160.
**Courant, R. and Hilbert, D.**, 1962. Methods of mathematical physics II, Interscience Publishers, New York, 830 pp.
**Deigaard, R.**, 1983. Formation of large bed undulations under waves and current - a stability analysis. Tech. Univ. Denmark, Inst. Hydrodyn. and Hydraulic Engrg., Prog. Rept. 59, p. 3-11.
**De Vriend, H.J.**, 1985. Flow formulation in mathematical models of 2DH morphological changes. Delft Hydr. Lab., TOW-rept. R1747-5, 64 pp.
**De Vriend, H.J.**, 1986. Two and three-dimensional mathematical modelling of coastal morphology. Delft Hydr. Lab., TOW-rept. H284-2, 36 pp. (Also: Delft Hydraulics Comm. no. 377).
**De Vriend, H.J.**, 1987a. 2DH mathematical modelling of morphological evolutions in shallow water. To appear in Coastal Engineering.
**De Vriend, H.J.**, 1987b. Analysis of 2DH morphological evolutions in shallow water. To appear in J. Geoph. Res. (Oceans).
**De Vriend, H.J., and Stive, M.J.F.**, 1986. Quasi-3D modelling of nearshore currents. JONSMOD '86 Colloquium, Delft, The Netherlands (to appear in special JONSMOD-issue of Coastal Engineering).
**De Vries, M.**, 1969. Solving river problems by hydraulic and mathematical models. Conf. on Simulation of Hydrodynamic Phenomena, Jablonna, Poland. (Also: Delft Hydr. Lab., Publ. no. 76-II).

REFERENCES (continued)

**Dingemans, M.W.**, 1985. Surface wave propagation over an uneven bottom; Evaluation of two-dimensional wave propagation models. Delft Hydr. Lab. Rept. no. W301-5, 117 pp.
**Dingemans, M.W., Radder, A.C. and De Vriend, H.J.**, 1987. Computation of the driving forces of wave-induced currents. JONSMOD '86 Colloquium, Delft, The Netherlands (submitted for publication).
**Fleming, C.A. and Hunt, J.N.**, 1976. Application of a sediment transport model. Proc. 15th ICCE, Honolulu, Hawaii, p. 1184-1202.
**Flokstra, C.**, 1981. Numerical aspects of calculating the bed level in river bends, Delft Hydr. Lab., Rept. R657-XII/W308 part II, 34 pp.
**Holman, R.A. and Bowen, A.J.**, 1982. Bars, bumps and holes: models for the generation of complex beach topography, J. Geoph.Res., 87, no. C1, p. 457-468.
**Koch, F.G. and Flokstra, C.**, 1981. Bed level computations for curved alluvial channels, Proc. XIXth IAHR Congress, New Delhi, Vol. 2, p. 357 (also: Delft Hydr. Lab., Publ. no. 240).
**Lin, P.N. and Shen, H.W.**, 1984. Two-D flows with sediment by characteristics method, J. Hydr. Engrg., 110, no. 5, p. 615-625.
**Longuet-Higgins, M.S.**, 1970. Longshore currents generated by obliquely incident sea waves. J. Geophys.Res., 75, p. 6778-6801.
**McAnally, W.H., Letter, J.V., Thomas, W.A. and Brogdon, N.J.**, 1984. Application of Columbia hybrid modelling system. J. Hydr. Engrg., 110, no. 5, p. 627-642.
**Stive, M.J.F.**, 1986. A model for cross-shore sediment transport. Proc. 20th ICCE, Taipei.
**Struiksma, N., Olesen, K.W., Flokstra, C. and De Vriend, H.J.**, 1985. Bed deformation in curved alluvial channels. J. Hydr. Res., 23, no. 1, p. 57-79.
**Tsujimoto, T. and Fukushima, T.**, 1985. Flow over the three-dimensional wavy bed - a linearized theory for bed instability analysis. Memoirs Fac. of Techn., Kanazawa Univ., Japan, 18, no. 2, p. 11-21.
**Van Banning, G.K.F.M., De Vriend, H.J. and Boer, S.**, 1987. Schematization and validation of 2DH mathematical models of coastal morphology. Coastal Sediments '87, New Orleans, Louisiana.
**Van de Graaff, J. and Van Overeem, J.**, 1979. Evaluation of sediment transport formulae in coastal engineering practice. Coastal Engineering, 3, p. 1-32.
**Watanabe, A.**, 1985. Three-dimensional predictive model of beach evolution around a structure. Symp. Water Wave Research, Hannover.
**Yamaguchi, M. and Nishioka, Y.**, 1984. Numerical simulation on the change of bottom topography by the presence of coastal structrues, Proc. 19th ICCE, Houston, Texas, p. 1732-1748.

APPENDIX I - ELABORATION OF THE CONSTITUENT EQUATIONS

If the right-hand member of the eikonal equation (3) is named $\kappa^2$, this equation can be replaced by

$$\frac{\partial\Phi}{\partial x} = \kappa \cos\Theta \text{ and } \frac{\partial\Phi}{\partial y} = \kappa \sin\Theta \tag{37}$$

Then the compatibility conditions for these phase function derivatives and the transport equation (4) can be elaborated to the linearized system

$$L_2(\Theta) - \frac{k^2}{\kappa^2}\frac{C_h}{h} L_1(h) + \frac{1}{2\kappa^2} L_1\left(\frac{\nabla^2 a}{a}\right) + \frac{C_h + C_{gh}}{2\kappa^2 ha} L_1\left(\frac{\partial a}{\partial x}\frac{\partial h}{\partial x} + \frac{\partial a}{\partial y}\frac{\partial h}{\partial y}\right) + \text{h.o.t.} = 0 \tag{38}$$

$$- L_1(\Theta) + \frac{2}{a} L_2(a) + \frac{1}{2\kappa^2} L_2 \left(\frac{\nabla^2 a}{a}\right) + \left[\frac{C_{gh}}{h} + \left(1 - \frac{k^2}{\kappa^2}\right) \frac{C_h}{h}\right] L_2(h) +$$
$$+ \frac{C_h + C_{gh}}{2\kappa^2 ha} L_2 \left(\frac{\partial a}{\partial x}\frac{\partial h}{\partial x} + \frac{\partial h}{\partial y}\frac{\partial h}{\partial y}\right) + \text{h.o.t.} = 0 \qquad (39)$$

in which $\nabla^2$ denotes the Lapalician and "h.o.t." indicates higher order terms in the derivatives of a and h. The operators $L_1$ and $L_2$ are defined as

$$L_1 = \cos\Theta \frac{\partial}{\partial x} + \sin\Theta \frac{\partial}{\partial y} \quad \text{and} \quad L_2 = \sin\Theta \frac{\partial}{\partial x} - \cos\Theta \frac{\partial}{\partial y} \qquad (40)$$

The flow equations (7) though (10) remain unaltered, except for the linearization of the bottom shear stress

$$\frac{\tau_{bx}}{\rho h} = \left(\frac{\tau_{bx}}{\rho h}\right)_o + (u-u_o)\, r_o + \left(u_t - u_{t_o}\right) \frac{u_o r_o}{u_{t_o}} R_u + (h-h_o) \frac{u_o r_o}{h_o} R_h \qquad (41)$$

and a similar expression for the y-component.

Substitution of the linearized expression for the sediment transport, (15), into (12) and (13) and subsequently into the sediment balance equation (14) yields, after some elaboration and making use of the equation of continuity (9), the advection/diffusion equation (18).

Equations (38) through (41) and (7) through (9) form a representation of the system in which all derivatives refer to the dependent variables $\Theta$, a, u, v, p and $z_b$ (or h).
If this system is linearized about the point ($\Theta_o, a_o, u_o, v=0, p_o, z_b=0$) in the solution space, i.e. if the x-axis is oriented downstream and the undisturbed bottom is horizontal, it can be written as

$$L_2(\Theta') + \frac{C_h}{h_o} L_1(z_b') + \frac{1}{2a_o k_o^2} L_1\left(\nabla^2 a'\right) = 0 \qquad (42)$$

$$- L_1(\Theta') - \frac{C_{gh}}{h_o} L_2(z_b') + \frac{2}{a_o} L_2(a') + \frac{1}{2a_o k_o^2} L_2 \left(\nabla^2 a'\right) = 0 \qquad (43)$$

$$u_o \frac{\partial u'}{\partial x} = - \frac{1}{\rho}\frac{\partial p'}{\partial x} - \left(1 + R_u\right) r_o u' - R_h \frac{u_o r_o}{h_o} h' \qquad (44)$$

$$u_o \frac{\partial v'}{\partial x} = - \frac{1}{\rho}\frac{\partial p'}{\partial y} - r_o v' \qquad (45)$$

$$\frac{\partial u'}{\partial x} + \frac{\partial v'}{\partial y} - \frac{u_o}{h_o}\frac{\partial z_b'}{\partial x} = 0 \qquad (46)$$

$$\frac{\partial z_b'}{\partial t} + \left(T_2 - T_1\right) \frac{S_{t_o}}{h_o}\frac{\partial z_b'}{\partial x} - \beta\, S_{t_o} \nabla^2 z_b' - T_2 \frac{S_{t_o}}{u_o}\frac{\partial v'}{\partial y} + T_3 \frac{S_{t_o}}{a_o}\frac{\partial a'}{\partial x} \qquad (47)$$

in which the primes indicate the deviation of the relevant quantity from the solution in point "o" in the solution space. The operators $L_1$ and $L_2$ are given by (40), with $\Theta = \Theta_o$.
The system (I.9) through (I.14) is subject to the harmonic analysis.